

RESEARCH ARTICLE

Effects of artemisinin antimalarials on Cytochrome P450 enzymes *in vitro* using recombinant enzymes and human liver microsomes: potential implications for combination therapies

Therese Ericsson, Jesper Sundell, Angelica Torkelsson, Kurt-Jürgen Hoffmann, and Michael Ashton

Unit for Pharmacokinetics and Drug Metabolism, Department of Pharmacology, Sahlgrenska Academy at the University of Gothenburg, Gothenburg, Sweden

Abstract

1. Cytochrome P450 enzyme system is the most important contributor to oxidative metabolism of drugs. Modification, and more specifically inhibition, of this system is an important determinant of several drug–drug interactions (DDIs).
2. Effects of the antimalarial agent artemisinin and its structural analogues, artemether, artesunate and dihydroartemisinin, on seven of the major human liver CYP isoforms (CYP1A2, 2A6, 2B6, 2C9, 2C19, 2D6 and 3A4) were evaluated using recombinant enzymes (fluorometric assay) and human liver microsomes (LC–MS/MS analysis). Inhibitory potency (IC_{50}) and mechanisms of inhibition were evaluated using nonlinear regression analysis. *In vitro–in vivo* extrapolation using the $[I]/K_i$ ratio was applied to predict the risk of DDI *in vivo*.
3. All compounds tested inhibited the enzymatic activity of CYPs, mostly through a mixed type of inhibition, with CYP1A2, 2B6, 2C19 and 3A4 being affected. A high risk of interaction *in vivo* was predicted if artemisinin is coadministered with CYP1A2 or 2C19 substrates.
4. With respect to CYP1A2 inhibition *in vivo* by artemisinin compounds, our findings are in line with previously published data. However, reported risks of interaction may be overpredicted and should be interpreted with caution.

Keywords

Artemether, artesunate, CYP enzymes, dihydroartemisinin, drug–drug interactions, inhibition

History

Received 28 November 2013
Revised 19 December 2013
Accepted 20 December 2013
Published online 8 January 2014

Introduction

Malaria, a life-threatening parasitic disease caused by protozoan parasites belonging to the *Plasmodium* genus, is one of the major public health challenges undermining development in the poorest countries in the world. Today the World Health Organization (WHO) recommends artemisinin-based combination therapies as the first-line treatment (WHO, 2010). The parent compound of the artemisinin class of drugs, artemisinin, is isolated from the plant *Artemisia annua*. In most countries the clinical use of artemisinin has been superseded by its semi-synthetic derivatives, such as artemether, artesunate and dihydroartemisinin. The unique feature of these compounds is the presence of an endoperoxide bridge as pharmacophore being essential for their antimalarial activity (van Agtmael et al., 1999b).

With today's comprehensive drug development, increased medical knowledge about diseases, and an increased life

expectancy, many patients undergo multiple-drug therapy, using more than one medication. Multiple-drug therapy poses several advantages, such as simultaneous treatment of conditions, or multidrug therapy for the treatment of complex chronic disorders, including hypertension, HIV, tuberculosis, malaria, cancer and neuropathic pain, resulting in a better treatment outcome compared to monotherapy (Backonja et al., 2006). However, coadministration of multiple drugs increases the risk for drug–drug interactions (DDIs), many of which are pharmacokinetically based and often involve drug metabolism (Shou et al., 2001). The most common cause of DDIs is modification of the enzymatic activity of Cytochrome P450 (CYP) enzymes, specifically through inhibitory effects. This enzymatic system constitutes a superfamily of isoforms that play the most important role in the oxidative phase I metabolism of drugs and, therefore have a significant impact on the severity of DDIs (Pelkonen et al., 2008). Inhibition of CYP enzymes *in vivo* may result in unexpected elevations in the plasma concentrations of concomitant drugs, leading to adverse effects. Therefore, regulatory authorities require preclinical (*in vitro*) and clinical (*in vivo*) interaction studies in the drug development process (FDA, 2012).

Artemisinin and artemether have previously been found to inhibit the activity of CYP2B6 in a non-time-dependent

Address for correspondence: Therese Ericsson, Unit for Pharmacokinetics and Drug Metabolism, Department of Pharmacology, Sahlgrenska Academy at the University of Gothenburg, Box 431, 405 30 Gothenburg, Sweden. Tel: +46 317863494. Fax: +46 317863164. E-mail: therese.ericsson@neuro.gu.se

fashion (Ericsson et al., 2012). The present study aimed to further investigate the effect of artemisinin, artemether, artesunate and dihydroartemisinin on the activity of seven of the major human liver CYP enzymes (CYP1A2, 2A6, 2B6, 2C9, 2C19, 2D6 and 3A4) *in vitro*. The CYP inhibitory potential of these endoperoxides was evaluated individually for each isoform, using recombinant enzymes (rCYP) and a fluorometric assay that utilizes biotransformation of pro-fluorescent substrates into fluorescent metabolites. Further, their inhibitory potential on the metabolic activity of the seven CYP enzymes were also evaluated simultaneously using a substrate cocktail approach using human liver microsomes (HLM) and LC–MS/MS analysis to simultaneously measure the formation of seven CYP-specific substrate metabolites.

Materials and methods

Materials

Pooled HLM (pool of 24 individuals, lot number 34689), BD supersomes, expressing CYP1A2, 2A6, 2B6, 2C9, 2C19, 2D6 and 3A4, respectively, and dibenzylfluorescein (DBF) were purchased from BD Bioscience (Woburn, MA). 3-[2-(*N,N*-Diethyl-*N*-methylammonium)-ethyl]-7-methoxy-4-methylcoumarin (AMMC), 7-benzyloxy-4-trifluoromethylcoumarin (BFC), 7-ethoxy-3-cyanocoumarin (CEC), 7-ethoxy-4-trifluoromethylcoumarin (EFC), 7-methoxy-4-trifluoromethylcoumarin (MFC), coumarine, 7-hydroxycoumarin, bupropion, hydroxybupropion, dextrorphan, dextropropranolol, mephenytoin, 4'-hydroxymephenytoin, midazolam, 1-hydroxymidazolam, phenacetin, acetaminophen, tolbutamide, 4-hydroxytolbutamide, chlorpropamide, furafylline, ketoconazole, quinidine, sulfaphenazole, tranlycypromine, glucose-6-phosphate dipotassium salt hydrate, NADP, glucose-6-phosphate dehydrogenase, magnesium chloride hexahydrate, potassium phosphate dibasic trihydrate and potassium phosphate monobasic were obtained from Sigma-Aldrich (St Louis, MO). Artemisinin was obtained from National Institute of Malaria, Parasitology and Entomology (NIMPE – Hanoi, Vietnam), artemether from Novartis (Basel, Switzerland), artesunate from the University of Algarve (Algarve, Portugal) and dihydroartemisinin was obtained from DK Pharma, Hanoi, Vietnam.

Fluorometric assay and conditions for recombinant enzymes incubations

Fluorescence-based P450 activity assays were performed by direct incubations of recombinant enzymes (rCYP1A2, 2A6, 2B6, 2C9, 2C19, 2D6 and 3A4) in microtiter plates (F96, NUNC, Thermo Scientific LPG LCD, Fischer Scientific, Gothenburg, Sweden) with selected substrates (Table 1). Stock solutions of test compounds, positive controls and substrates were prepared in acetonitrile with a final acetonitrile concentration in all wells <2% v/v. All incubations were conducted at 37 °C with a final working volume of 200 µL/well, containing either phosphate buffer, pH 7.4 (rCYP1A2, 2B6, 2C9, 2C19, 2D6 and 3A4) or Tris buffer, pH 7.4 (rCYP2A6; inhibited by phosphate; Stresser, 2004) and an NADPH-regenerating system (1.3 mM NADP⁺, 3.3 mM G-6-P, 3.3 mM MgCl₂ and 0.4 U/mL G-6-P-D for rCYP1A2, 2B6, 2C9 and 2D6; 8.2 µM NADP⁺, 0.41 mM G-6-P, 0.14 mM MgCl₂ and 0.4 U/mL G-6-P-D for rCYP2A6, 2C19 and 3A4). Test compounds, positive control or vehicle in buffer and NADPH-regenerating system were pre-incubated (37 °C) for 10 min in a 96-well plate. Reactions were initiated by the addition of an enzyme/substrate solution (final substrate concentration approximately equal to their respective *K_m*; Stresser, 2004) and were allowed to run for the respective incubation time (Table 1). Reactions were stopped by the addition of 75 µL stop solution containing Tris–acetonitrile, 20:80 v/v (or 2 M NaOH for the DBF reaction with CYP3A4). Fluorescence was measured using a Tecan Infinite F200 fluorometer (Tecan Nordic AB, Mölndal, Sweden), with the intensity of the response used as a measure of the metabolite formation rate. The percentage activity remaining was calculated by comparing the inhibited activity (fluorescence intensity) with non-inhibited controls.

Inhibition studies with rCYP

Single point inhibition assay

The enzymatic activities of rCYP1A2, 2A6, 2B6, 2C9, 2C19, 2D6 and 3A4 were evaluated in the absence and presence of artemisinin (80 µM), artemether (80 µM), artesunate (80 µM) dihydroartemisinin (80 µM) or positive controls (30 µM furafylline, rCYP1A2; 8 µM tranlycypromine, rCYP2A6; 40 µM tranlycypromine, rCYP2B6; 3 µM sulfaphenazole,

Table 1. Experimental conditions for the single point inhibition assay and the IC₅₀ assay with recombinant enzymes.

P450 isoform	Substrate/metabolite	[Substrate] (µM)	Enzyme (nmol/L)	Buffer (mM)	Incubation time (min)
1A2	CEC/CHC	5	2.5	KPO ₄ (100)	15
2A6	COU/HC	3	5	TRIS (100)	30
2B6	EFC/HFC	2.5	5	KPO ₄ (100)	30
2C9	MFC/HFC	75	20	KPO ₄ (25)	45
2C19	CEC/CHC	25	5	KPO ₄ (50)	30
2D6	AMMC/AMHC	1.5	7.5	KPO ₄ (100)	15
3A4	BFC/HFC	50	5	KPO ₄ (200)	30
3A4	DBF/Fluorescein	1	1	KPO ₄ (200)	10

Abbreviations: AMMC, 3-[2-(*N,N*-diethyl-*N*-methylammonium)-ethyl]-7-methoxy-4-methylcoumarin; BFC, 7-benzyloxy-4-trifluoromethylcoumarin; CEC, 7-ethoxy-3-cyanocoumarin; COU, coumarin; DBF, dibenzylfluorescein; EFC, 7-ethoxy-4-trifluoromethylcoumarin; MFC, 7-methoxy-4-trifluoromethylcoumarin; AMHC, 3-[2-(*N,N*-diethyl-*N*-methylammonium)ethyl]-7-hydroxy-4-methylcoumarin; HFC, 7-hydroxy-4-trifluoro-methylcoumarin; CHC, 7-hydroxy-3-cyanocoumarin; HC, 7-hydroxycoumarin.

rCYP2C9; 55 μM tranylcypropromine, rCYP2C19; 0.2 μM quinine, rCYP2D6; 0.2 μM ketoconazole, rCYP3A4). Test compound concentration was set to a level that was expected to produce a relevant inhibitory effect in the event of enzyme inhibition. After pre-incubation (37 °C), reactions were initiated by the addition of an enzyme/substrate solution, allowed to run for recommended incubation times, before termination followed by fluorescence measuring as described above. Experimental conditions are shown in Table 1.

IC₅₀ determinations

Based on the results from the single point inhibition assay described above, the enzymatic activity of inhibited enzymes (rCYP1A2, 2B6, 2C19 and 3A4) was further investigated in the absence and presence of multiple concentrations of test compound (0.1–240 μM). After pre-incubation (37 °C), reactions were initiated by the addition of an enzyme/substrate solution, allowed to run for the respective incubation time, before termination followed by fluorescence measuring as described above. Experimental conditions are shown in Table 1.

Determination of inhibition mechanism and K_i

The recombinant enzyme/test compound combinations that showed inhibition in the IC₅₀ assay described above, were further investigated to estimate the inhibition constant (K_i) and determine the mechanism of inhibition. Multiple concentrations of substrate (CEC for rCYP1A2 and 2C19; EFC for rCYP2B6) were incubated in absence and presence of artemisinin test compounds (three concentrations). The NADPH-regenerating system was added as cofactor and the reactions were initiated by the addition of recombinant enzymes and were allowed to run for an appropriate time before termination followed by fluorescence measuring as described above. Experimental conditions are shown in Table 2.

Cocktail incubation with HLM

To assess the enzymatic activity of CYP1A2, 2A6, 2B6, 2C9, 2C19, 2D6 and 3A4 in microsomal incubations, a substrate cocktail inhibition assay using HLM followed by LC–MS/MS analysis for the quantification of formed metabolites was used. The method was developed based on modifications of a previously described assay by Kim et al. (2005). CYP P450 enzyme-specific substrates were divided into two sets of cocktail doses. Set A included phenacetin (CYP1A2), coumarin (CYP2A6), S-mephenytoin (CYP2C19), dextromethorphan (CYP2D6) and midazolam (CYP3A4), and set B included bupropion (CYP2B6) and tolbutamide (CYP2C9). The final substrate concentrations used were approximately equal to their respective K_m value (Table 3). All incubations were conducted in a 96-well plate format at 37 °C with a final working volume of 200 μL /well, containing 0.1 M phosphate buffer (pH 7.4), NADPH-regenerating system (1.3 mM NADP⁺, 3.3 mM G-6-P, 3.3 mM MgCl₂, 0.4 U/mL G-6-P-D), 0.25 mg/mL microsomal protein, substrates (set A or set B) and a test compound, positive controls or vehicle (no inhibitor). Due to inhibition of the 4-hydroxylation of tolbutamide by methanol (>1%), and the inhibition of 7-hydroxylation of coumarin by acetonitrile (<1%) (Chauret et al., 1998), test compounds and positive controls were dissolved in methanol for incubations containing substrate set A and in acetonitrile for incubations containing substrate set B (final solvent concentration <1%).

Test compounds, positive control or vehicle in phosphate buffer and NADPH-regenerating system were pre-incubated (37 °C) for 10 min. The reactions were initiated by the addition of a pre-warmed (37 °C) solution containing HLM and substrates (set A or set B). Incubations were allowed to run for 20 min before being terminated by placing the plates on ice and adding 200 μL of cold acetonitrile containing 20 μM chlorpropamide as an internal standard (IS).

Table 2. Experimental conditions for the K_i assay with recombinant enzymes.

P450 isoform	Enzyme (nmol/L)	Substrate (μM)	Buffer (mM)	Incubation time (min)	Artemisinin test compound (μM) ^a			
					ART	ARM	ARS	DHA
1A2	2.5	CEC (0.02–10)	KPO ₄ (100)	15	3, 10, 30	NI ^b	NI ^b	15, 40, 120
2B6	5	EFC (0.25–100)	KPO ₄ (100)	15	5, 50, 100	5, 50, 100	NI ^b	NI ^b
2C19	5	CEC (1.5–80)	KPO ₄ (50)	30	3, 10, 30	6, 20, 60	NI ^b	10, 30, 90

^aThree concentrations of artemisinin test compound used in each assay run; ART, artemisinin; ARM, artemether; ARS, artesunate; DHA, dihydroartemisinin.

^bNo inhibition observed in the single point inhibition assay; K_i assay not applied.

Table 3. Experimental conditions and MRM parameters for the P450 probe substrates and IS used in the cocktail assays.

P450 isoform	Substrate	Concentration (μM)	Metabolite	Transition (<i>m/z</i>)	Collision energy (eV)
1A2	Phenacetin	50	Acetaminophen	152 > 120	24
2A6	Coumarin	5	7-Hydroxycoumarin	163 > 107	22
2B6	Bupropion	50	Hydroxybupropion	256 > 238	16
2C9	Tolbutamide	100	4-Hydroxytolbutamide	287 > 89	16
2C19	S-Mephenytoin	100	4'-Hydroxymephenytoin	235 > 150	(25) ^a
2D6	Dextromethorphan	5	Dextrorphan	258 > 157	10
3A4	Midazolam	5	1-Hydroxymidazolam	342 > 203	14
IS	Chlorpropamide			277 > 175	12 (24) ^a

^aMRM parameter values for the 4'-hydroxymephenytoin LC–MS/MS method using an API 4000 instrument.

The samples were centrifuged at 3000 *g* for 20 min in room temperature. Corresponding supernatants from set A and set B were pooled together and analyzed by LC–MS/MS along with calibration standards.

Calibration standards were prepared at six concentrations in a blank microsomal incubation mixture. The concentration range differed depending on the sensitivity of the method for each metabolite; acetaminophen 0.05–25 μM , 7-hydroxycoumarin 0.005–2.5 μM , hydroxybupropion 0.01–50 μM , 4-hydroxytolbutamide 0.01–50 μM , 4'-hydroxymephenytoin 0.1–50 μM , dextrorphan 0.005–2.5 μM and 1-hydroxymidazolam 0.005–2.5 μM .

Inhibition studies with HLM

Single point inhibition assay

The enzymatic activities of CYP1A2, 2A6, 2B6, 2C9, 2C19, 2D6 and 3A4 in HLM were evaluated in the absence and presence of artemisinin (80 μM), artemether (80 μM), artesunate (80 μM), dihydroartemisinin (80 μM) and positive controls (30 μM furafylline, CYP1A2; 50 μM tranlycypromine, CYP2A6; 50 μM tranlycypromine, CYP2B6; 3 μM sulfaphenazole, CYP2C9; 50 μM tranlycypromine, CYP2C19; 0.2 μM quinidine, CYP2D6; 5 μM ketoconazole, CYP3A4). After pre-incubation (37 °C), reactions were initiated by the addition of a HLM/substrate start solution, allowed to run for 20 min before being terminated and samples processed as described above.

IC₅₀ determinations

Based on the results from the single point inhibition assay described above, the enzymatic activity of inhibited enzymes (CYP1A2, 2B6, 2C19 and 3A4) was further investigated in the absence and presence of multiple concentrations of test compounds (0.1–400 μM). After the pre-incubation (37 °C) the reactions were initiated by the addition of a HLM/substrate start solution, allowed to run for 20 min before terminated and samples processed as described above.

LC–MS/MS method for cocktail incubations

An API 3000 triple quadrupole mass spectrometer (Applied Biosystems/MDS SCIEX, Foster City, CA) equipped with an electrospray ionization (ESI) interface operated in the positive ion mode and multiple reaction monitoring (MRM) was used for quantification of formed metabolites in the pooled HLM cocktail incubation samples. The mass spectrometric conditions were optimized for each metabolite by infusing a 0.1–1 μM solution at a flow rate of 10 $\mu\text{L}/\text{min}$ using a Harvard infusion pump (Harvard Apparatus, Holliston, MA) connected directly to the mass spectrometer. The ESI temperature was maintained at 400 °C and the ESI voltage was set to 5000 V. High purity nitrogen was used as nebulizer gas (9 psi), curtain gas (6 psi) and collision gas (8 psi). MRM transitions (*m/z*) and the optimized collision energies determined for each metabolite and IS are listed in Table 3.

Samples (5 μL) were injected onto a Luna 5 μm C18 column (30 mm \times 2.00 mm) (Phenomenex, Torrance, CA), protected by a SecurityGuard C18 HPLC column

(Phenomenex ApS, DK), using a Perkin Elmer 200 Series autoinjector connected to two Perkin Elmer 200 Series pumps (Perkin Elmer, Waltham, MA). The mobile phase consisted of 0.1% formic acid in water (A) and 0.1% formic acid in acetonitrile (B). Analytes were eluted using a gradient flow (0.2 mL/min), with mobile phase B linearly increasing from 10% to 80% during 1 min, held at 80% for an additional 2 min and then linearly decreasing to 10% over 30 s for re-equilibration. Samples were run at room temperature with a total analysis time of 6.5 min.

Data acquisition and quantification were performed using Analyst 1.4 (Applied Biosystems/MDS SCIEX). The percentage activity remaining was calculated by comparing the calculated substrate metabolite concentrations of inhibited samples with the calculated substrate metabolite concentrations of non-inhibited control samples.

LC–MS/MS method for 4'-hydroxymephenytoin

To enable measurements of low concentrations of 4'-hydroxymephenytoin present in the pooled HLM cocktail incubation samples, the assay was further optimized using an API 4000 triple quadrupole mass spectrometer equipped with an ESI interface (Applied Biosystems/MDS SCIEX). The system was operated in the positive ion mode and tuned for the MRM for the detection of 4'-hydroxymephenytoin and IS chlorpropamide. The ESI temperature was maintained at 225 °C and the ESI voltage was set to 5500 V. Collision gas was set to 12 psi, curtain gas to 17 psi, and ion source gas one and two to 12 and 19 psi, respectively. The MRM transitions (*m/z*) and collision energies determined for 4'-hydroxymephenytoin and IS are listed in Table 3.

A temperature-controlled CTC PAL Autosampler (Leap Technologies, Carrboro, NC) set at 6 °C was used to inject sample (10 μL) onto the same LC columns as described above. The mobile phase consisted of 0.1% formic acid in water (A) and 0.1% formic acid in acetonitrile (B). Two Perkin Elmer 200 Series pumps were used to generate a gradient flow (0.2 mL/min), with mobile phase B held at 25% during 1.5 min, before linearly increasing to 95% over 0.1 min, and held at this value for an additional 1.5 min, before finally linearly decreasing to 25% over 0.1 min for re-equilibration. Samples were run at room temperature with a total analysis time of 5.5 min. During the first 0.6 min after injection, the LC eluent was diverted to waste to minimize contamination of the ion source.

Data acquisition was performed using Analyst 1.4. The percentage remaining activity was calculated by comparing the analyte/IS ratio of inhibited samples with the analyte/IS ratio of non-inhibited control samples. Due to very low amount of formed 4'-hydroxymephenytoin in the pooled HLM cocktail incubation samples, only the analyte/IS ratio was used.

Data analysis

Single point inhibition assay

The percentage remaining activity was calculated by comparing the formation of metabolite in each sample relative to the average metabolite formation in control samples.

IC₅₀ determinations

The formation of metabolite in each sample relative to the average non-inhibited control (percentage remaining activity) was calculated and IC₅₀ values were estimated by fitting either an inhibitory effect I_{\max} model (Equation (1); $\gamma = 1 = \text{fixed}$) or an inhibitory effect sigmoid I_{\max} model (Equation (1); γ estimated) to pooled ($n = 4$) and unweighted data using Phoenix[®] WinNonlin[®] 6.2 (Pharsight Corp, Mountain View, CA).

$$\% \text{ Remaining activity} = E_0 - \frac{I_{\max} \times [I]^\gamma}{IC_{50}^\gamma + [I]^\gamma}, \quad (1)$$

where E_0 represents maximal enzyme activity in the absence of inhibitor, I_{\max} is the maximum drug induced inhibition of the enzyme activity, $[I]$ is the concentration of the inhibitory drug and γ describes the sigmoidicity of the relationship. Model discrimination was based on evaluation of parameter estimate precisions (relative standard error), correlation between observed and predicted variable values, residual plots and the Akaike information criterion.

Determination of inhibition mechanism and K_i

To evaluate the mechanism of rCYP1A2, 2B6 and 2C19 inhibition apparent V_{\max} and K_m values in the absence and presence of increasing concentrations of inhibitors (see Table 2) were estimated. A single-site Michaelis–Menten equation, $V = (V_{\max} \times [S]) / (K_m + [S])$, was fitted to mean metabolite formation (fluorescence intensity, $n = 4$) of control and inhibited samples versus substrate concentration, using Sigma Plot 2001, Enzyme Kinetics Module 1.1 (SPSS Science Ltd, Birmingham, UK). To further investigate the mechanism of inhibition and to estimate K_i values, a model-based approach with nonlinear regression analysis was adopted. Enzyme kinetic parameters (K_m , V_{\max} and K_i) for recombinant enzymes were estimated by simultaneously fitting eight kinetic equations, describing different mechanisms of inhibition, to mean metabolite formation (fluorescence intensity, $n = 4$) in the absence and presence of increasing concentration of inhibitors versus substrate concentration, using Sigma Plot 2001, Enzyme Kinetics Module 1.1. Discrimination between competing models was performed as described above.

Predicted change in drug exposure in vivo

To evaluate the clinical relevance of a potential enzyme inhibition, a static model using the $[I]/K_i$ ratio was applied, where $[I]$ is the inhibitor concentration and K_i represents the inhibition constant. The degree of interaction is expressed as the increase in the exposure, represented by the area under the plasma concentration–time curve (AUC), of a substrate in the presence of an interacting, inhibitory drug. Assuming that the inhibited metabolic pathway is the only route of metabolism of the substrate, the ratio of AUCs is dependent on the $[I]/K_i$ ratio, explained by Equation (2).

$$\frac{AUC_1}{AUC} = 1 + \frac{[I]}{K_i}, \quad (2)$$

where AUC_1 and AUC stand for the area under the drug plasma concentration–time curve in the presence and absence

of inhibitor, respectively. An AUC ratio above 2 indicates a high risk of DDIs, ratios between 1.1 and 2 indicate a medium risk while an AUC ratio below 1.1 indicates a low risk of interactions (Ito et al., 2004). The AUC ratios were calculated based on the maximum unbound systemic concentrations of the inhibitor ($[I]_{\max,u}$) and the maximum unbound concentrations of the inhibitor at the inlet to the liver ($[I]_{\max,inlet,u}$; calculated as proposed by Ito et al. (1998)). *In vivo* concentrations and parameters used to calculate $[I]_{\max,u}$ and $[I]_{\max,inlet,u}$ for artemisinin (Alin et al., 1996; Ashton et al., 1998b; Augustijns et al., 1996; Sidhu et al., 1998), artemether (Colussi et al., 1999; Ezzet et al., 1998; van Agtmael et al., 1999a; White et al., 1999) and dihydroartemisinin (Batty et al., 2004; Na-Bangchang et al., 2004), respectively, were taken from literature.

Results

LC–MS/MS method for cocktail incubations

The cocktail inhibition assay using HLM and LC–MS/MS analysis for the quantification of CYP specific substrate metabolites, previously described by Kim et al. (2005), was optimized on an API 3000 MS system (Applied Biosystems/MDS SCIEX, Foster City, CA). With the current instruments and analytical settings, the method was sensitive to successfully analyse all calibration standards and incubation samples for the quantification of acetaminophen (CYP1A2), 7-hydroxycoumarin (CYP2A6), hydroxybupropion (CYP2B6), 4-hydroxytolbutamide (CYP2C9), dextropran (CYP2D6), 1-hydroxymidazolam (CYP3A4), using chlorpropamide as IS. HPLC chromatograms from the analysis with the mass spectrometer in MRM mode of a representative HLM sample are available as supplemental information.

LC–MS/MS method for 4'-hydroxymephenytoin

Due to the low concentrations of 4'-hydroxymephenytoin in the HLM cocktail incubation samples, a method was optimized using an API 4000 LC/MS instrument for the determination of the metabolite. Concentrations of 4'-hydroxymephenytoin could not be fully determined because metabolite levels in the samples were below the lowest calibration standard. Therefore, the analyte/IS ratio was used to assess the percent remaining CYP2C19 activity, by comparing the ratios of samples with the mean ratio of control samples. To evaluate the precision of the analyte/IS ratio approach, two control HLM incubation samples were injected six times in sequence and analyzed. A mean analyte/IS ratio ($n = 6$) for each sample could be calculated with a coefficient of variation (CV%) of 6.7 and 8.9, respectively, indicating high precision. MRM chromatograms from the analysis of a representative calibration standard are available as supplemental information.

Single point inhibition assay

Results for incubations with a single high concentration of test compounds or positive controls are listed in Table 4. Artemisinin inhibited CYP1A2, 2B6 and 2C19 activities in both *in vitro* systems tested, while artemether showed inhibitory effects on recombinant and microsomal CYP2B6

Table 4. Percentage remaining activity after incubation with 80 μM test compound or positive controls (see ‘‘Materials and methods’’). Data is represented as mean value ± standard deviation ($n = 4$).

CYP isoform	ART	ARM	ARS	DHA	Positive control
1A2: rCYP	7.8 ± 0.9	NI	NI	27.7 ± 2.5	7.7 ± 0.5
HLM	9.1 ± 1.6	NI	41.7 ± 1.2	15.7 ± 0.5	4.1 ± 0.3
2A6: rCYP	NI	NI	NI	NI	6.3 ± 1.7
HLM	NI	NI	NI	NI	2.9 ± 0.5
2B6: rCYP	9.6 ± 0.7	3.8 ± 0.8	NI	NI	36.1 ± 3.3
HLM	11.4 ± 0.8	4.1 ± 1.2	NI	NI	11.2 ± 0.9
2C9: rCYP	NI	NI	NI	NI	12.2 ± 1.5
HLM	NI	NI	NI	NI	22.5 ± 0.6
2C19: rCYP	21.5 ± 1.9	14.0 ± 1.6	NI	36.5 ± 2.4	15.3 ± 1.5
HLM	29.5 ± 0.2	24.7 ± 6.9	NI	42.7 ± 9.0	10.6 ± 0.1
2D6: rCYP	NI	NI	NI	NI	3.7 ± 0.4
HLM	NI	NI	NI	NI	16.0 ± 1.0
3A4: rCYP	NI ^a	NI ^a	NI ^a	NI ^a	15.8 ± 1.8
HLM	57.4 ± 0.5	59.5 ± 2.2	NI	NI	1.4 ± 0.4

Abbreviations: ART, artemisinin; ARM, artemether; ARS, artesunate; DHA, dihydroartemisinin; NI, no inhibition observed.

^aNo observed effect on the rCYP3A4 catalyzed dealkylation of DBF, but a slight activation (percentage remaining activity > 100%) of the BFC dealkylation.

and 2C19. Artesunate inhibited microsomal CYP1A2, while dihydroartemisinin inhibited CYP1A2 and 2C19 activity in both recombinant and microsomal enzymes. The activity of CYP3A4 was studied using three different substrates: BFC and DBF in recombinant enzymes, and midazolam in HLM. No effect on the rCYP3A4 catalyzed DBF dealkylation was observed for any of the artemisinin compounds tested at concentrations of 80 μM. However, all test compounds showed a slight activation (percentage remaining activity > 100%) of the rCYP3A4-mediated dealkylation of BFC, while artemisinin and artemether inhibited CYP3A4 activity and the hydroxylation of midazolam in HLM. As expected, all the positive controls showed inhibitory effects on their respective enzymes.

IC₅₀ determinations

The inhibitory potency of artemisinin, artemether, artesunate and dihydroartemisinin on affected enzymes from the single point inhibition assay were evaluated further by estimating IC₅₀ values based on Equation (1). Representative inhibition curves are presented in Figure 1. No major differences between the two assays were seen and estimated IC₅₀ values obtained in recombinant enzymes and HLM were in the same order of magnitude (Table 5). The most potent *in vitro* inhibitions observed were on CYP2B6 by artemether (IC₅₀ estimated to 2.4 and 2.9 μM in rCYP2B6 and HLM, respectively), and on CYP1A2 by artemisinin (IC₅₀ estimated to 6.3 and 1.4 μM in rCYP2B6 and HLM, respectively).

Determination of inhibition mechanism and K_i

Using recombinant enzymes, the mechanisms of artemisinin test compounds inhibition on rCYP1A2, 2B6 and 2C19 activities, respectively, were evaluated by the estimation of apparent V_{max} values and apparent K_m values in the absence and presence of increasing inhibitor concentrations using a single-site Michaelis–Menten equation. As shown in Figure 2 the inhibition of rCYP1A2 by artemisinin and dihydroartemisinin, as well as the inhibition by artemisinin and

artemether on rCYP2B6 and rCYP2C19, were characterized by decreasing apparent V_{max} values and increasing apparent K_m values with increasing inhibitor concentrations, indicating mixed modes of inhibition. The inhibition of rCYP2C19 by dihydroartemisinin did show a decrease in apparent V_{max} values but unchanged apparent K_m value with increasing inhibitor concentrations, indicating a noncompetitive inhibition mechanism.

Consistent with the above results, the inhibition of rCYP1A2 by artemisinin and dihydroartemisinin, as well as the inhibition of both rCYP2B6 and rCYP2C19 by artemisinin and artemether were best described by a partial mixed inhibition model (Equation (3)). The inhibitory effect by dihydroartemisinin on rCYP2C19 was best described by the partial noncompetitive inhibition model (Equation (4)).

$$V = V_{\max} * \frac{(1 + ((\beta * I)/(\alpha * K_i)))/(1 + (I/(\alpha * K_i)))}{1 + (K_m/S) * (1 + (I/K_i))/(1 + (I/(\alpha * K_i)))}, \quad (3)$$

$$V = \frac{V_{\max}}{(1 + \frac{K_m}{S}) * (1 + \frac{I}{K_i}) / (1 + \frac{I * \beta}{K_i})} \quad (4)$$

where V stands for the rate of metabolite formation, V_{\max} represents the maximal rate of metabolite formation, S and I are the substrate and inhibitor concentration, respectively and K_m is a constant associated with the enzyme affinity for a substrate. In mixed type inhibition, the inhibitor (I) and the substrate (S) bind to different sites of the enzyme (E) and the binding of one affects the binding affinity for the other. The change in binding affinity (increase in apparent K_m) for the substrate is included in the equation by the term α , and the term β defines the decrease in apparent V_{\max} for partial mixed and noncompetitive inhibition, respectively. Observed and predicted values based on Equations (3) and (4) are presented in Figures 3 for artemisinin, artemether and dihydroartemisinin on rCYP1A2, 2B6 and 2C19 activity, respectively. Estimated parameter values are presented in Table 6.

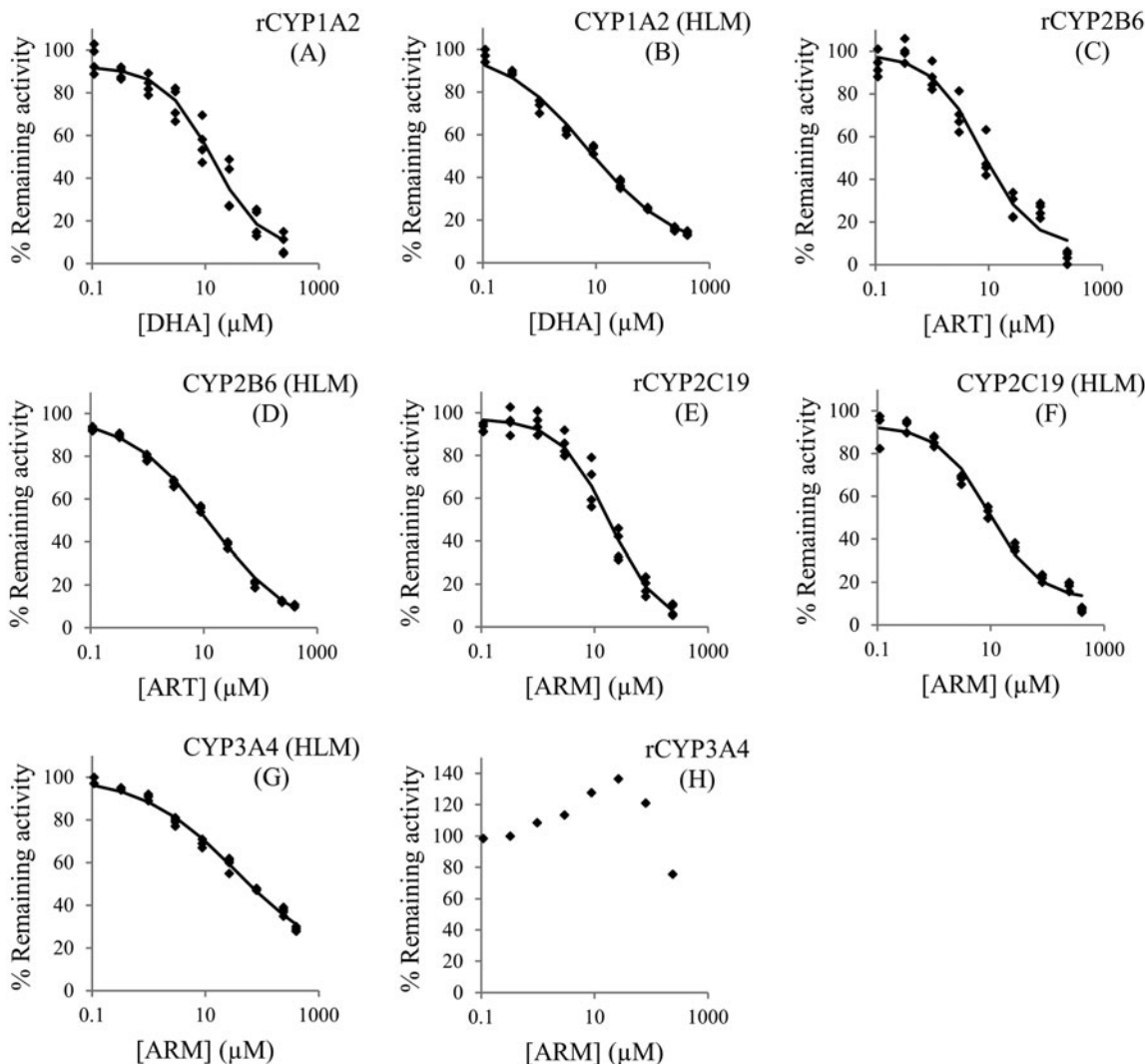


Figure 1. Inhibition of CYP activities by increasing concentrations (0.1–240 μM rCYP, 0.1–400 μM HLM) of artemisinin (ART), artemether (ARM) and dihydroartemisinin (DHA) using individual substrates in recombinant enzymes and the substrate cocktail in HLM (see ‘‘Materials and methods’’). Results in graphs A–G are presented as observed experimental data (diamonds, $n = 4$) with the lines obtained from fitting Equation (1) by nonlinear regression. Results in graph H are presented as mean values of observed experimental data (diamonds, $n = 4$). Y-axis indicates the percentage of vehicle control. Inhibition of rCYP1A2 (A) and microsomal CYP1A2 (B) by dihydroartemisinin; inhibition of rCYP2B6 (C) and microsomal CYP2B6 (D) by artemisinin; inhibition of rCYP2C19 (E) and microsomal CYP2C19 (F) by artemether; inhibition of microsomal CYP3A4 by artemether (G), and activation/inhibition of rCYP3A4 catalyzed BFC dealkylation by artemether (H).

Table 5. IC_{50} values (μM) estimated by nonlinear regression for the inhibition of recombinant (rCYP) and microsomal (HLM) CYP1A2, 2B6, 2C19 and 3A4 activity by artemisinin, artemether, artesunate and dihydroartemisinin, respectively.

CYP isoform	ART	ARM	ARS	DHA
1A2: rCYP	6.3 ± 0.8^b	NE	NE	13.1 ± 2.4^a
HLM	1.4 ± 0.2^b	NE	12.8 ± 1.2^b	7.2 ± 1.1^b
2B6: rCYP	7.4 ± 1.4^a	2.4 ± 0.5^b	NE	NE
HLM	12.8 ± 1.1^2	2.9 ± 0.4^b	NE	NE
2C19: rCYP	15.0 ± 4.5^a	18.3 ± 2.3^a	NE	21.9 ± 3.8^a
HLM	10.9 ± 0.9^b	9.2 ± 1.1^a	NE	13.0 ± 1.3^b
3A4: rCYP	NE	NE	NE	NE
HLM	18.1 ± 2.5^b	34.4 ± 10.3^b	NE	NE

Abbreviations: ART, artemisinin; ARM, artemether; ARS, artesunate; DHA, dihydroartemisinin; NE, not estimated.

^aParameter estimate \pm SE based on Equation (1) ($\gamma = 1$) ($n = 4$); values in molar unit (μM).

^bParameter estimate \pm SE based on Equation (1) (γ estimated) ($n = 4$); values in molar unit (μM).

Predicted change in drug exposure *in vivo*

Based on the static model (Equation (2)), AUC ratios were calculated using $[I]_{\text{max},u}$ or $[I]_{\text{max},\text{inlet},u}$ and K_i values for artemisinin, artemether and dihydroartemisinin on CYP1A2, 2B6 and 2C19, respectively, as estimated in this study (Table 7). For artemisinin, a high risk for DDI *in vivo* was predicted if coadministered with a CYP1A2 or 2C19 substrate, while a medium risk was predicted with a CYP2B6 substrate. The predicted risk for dihydroartemisinin to change the exposure of a CYP1A2 substrate resulting in DDI was medium when using $[I]_{\text{max},\text{inlet},u}$, but low when using $[I]_{\text{max},u}$. For dihydroartemisinin on CYP2C19, and artemether on CYP2B6 and 2C19, respectively, the predicted risks for DDI were low.

Discussion

In the present study the inhibition capacities of artemisinin, artemether, artesunate and dihydroartemisinin on seven

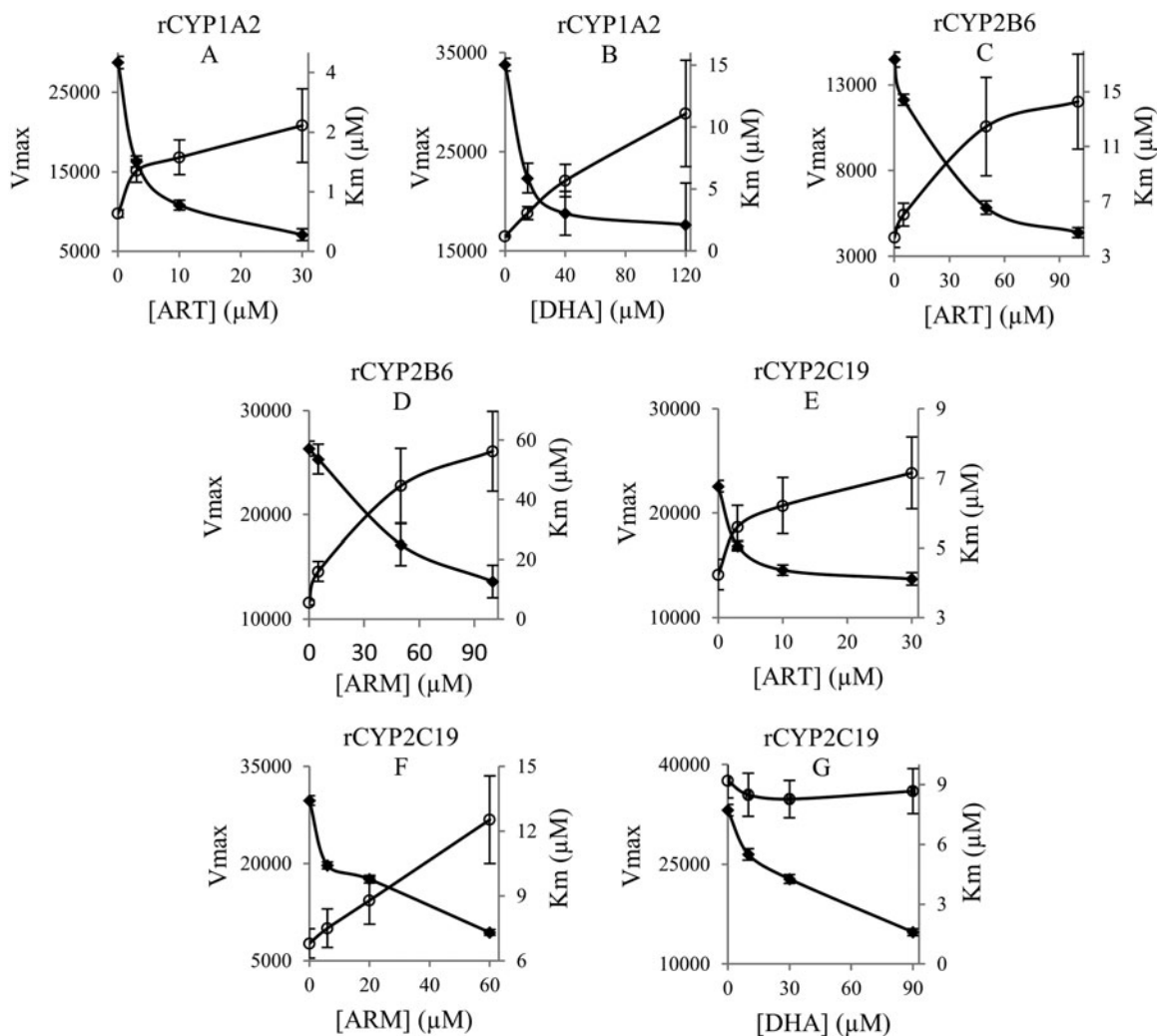


Figure 2. Apparent V_{max} values (closed diamonds) and apparent K_m values (open circles) for the formation of fluorescent metabolites (see *Materials and methods*) in recombinant enzymes in the absence and presence of increasing concentrations of artemisinin (ART), artemether (ARM) and dihydroartemisinin (DHA). Apparent kinetic parameters are estimated by nonlinear regression (Michaelis–Menten equation), and data are presented as parameter estimates \pm SE ($n = 4$). Maximal metabolite formation rates (V_{max}) are represented by the fluorescence intensity. Inhibition of rCYP1A2 by artemisinin (A) and dihydroartemisinin (B); inhibition of rCYP2B6 by artemisinin (C) and artemether (D); inhibition of rCYP2C19 by artemisinin (E), artemether (F) and dihydroartemisinin (G).

human drug-metabolizing CYPs have been investigated using two *in vitro* assays; the fluorescent probe method with recombinant human CYP enzymes, and a substrate cocktail assay in HLM based on LC–MS/MS. The performances in identifying potential enzyme inhibition of these *in vitro* tests, in addition to the conventional single substrate assay, have been systematically compared by Turpeinen et al. (2006). All three assays yielded remarkably similar results, and the fluorescence based technology and the cocktail approach were found to be suitable for measuring the inhibition of CYP activity compared to the traditional single substrate assay. In the present study, the estimated IC_{50} values were generally of the same order of magnitude in the two assays used. The cocktail approach offers the advantage of testing multiple enzymes in one study, compared to the fluorometric assay where each CYP isoform is evaluated separately. However, limitations of the cocktail approach include the requirement of high selective and sensitive analytical methods and the risk of interferences between compounds during analysis.

All four tested artemisinin compounds were shown to inhibit CYP enzymes, with CYP1A2, 2B6, C19 and 3A4 being affected. This is in line with previously published data showing inhibition on the given CYP isoforms by artemisinins. CYP1A2 has been reported to be inhibited by artemisinin and dihydroartemisinin in recombinant enzymes and HLM (Bapiro et al., 2001; He et al., 2007). The inhibitory effect on CYP1A2 activity has also been confirmed in healthy subjects (Asimus et al., 2007; Bapiro et al., 2005), with an inhibition of the enzymatic activity *in vivo* by 66% exerted by artemisinin (Bapiro et al., 2005). These *in vivo* data support our findings with a predicted medium to high risk for DDIs with dihydroartemisinin and artemisinin, respectively, on CYP1A2. CYP2B6 activity has been reported to be inhibited by artemisinin compounds in several *in vitro* systems, including recombinant enzymes, HLM and primary hepatocytes (Ericsson et al., 2012; Xing et al., 2012). The enzymatic activity of recombinant and microsomal CYP2C19 is subject to inhibition by artemisinin and dihydroartemisinin (Bapiro et al., 2001). Finally, a minor, but negligible, inhibitory effect

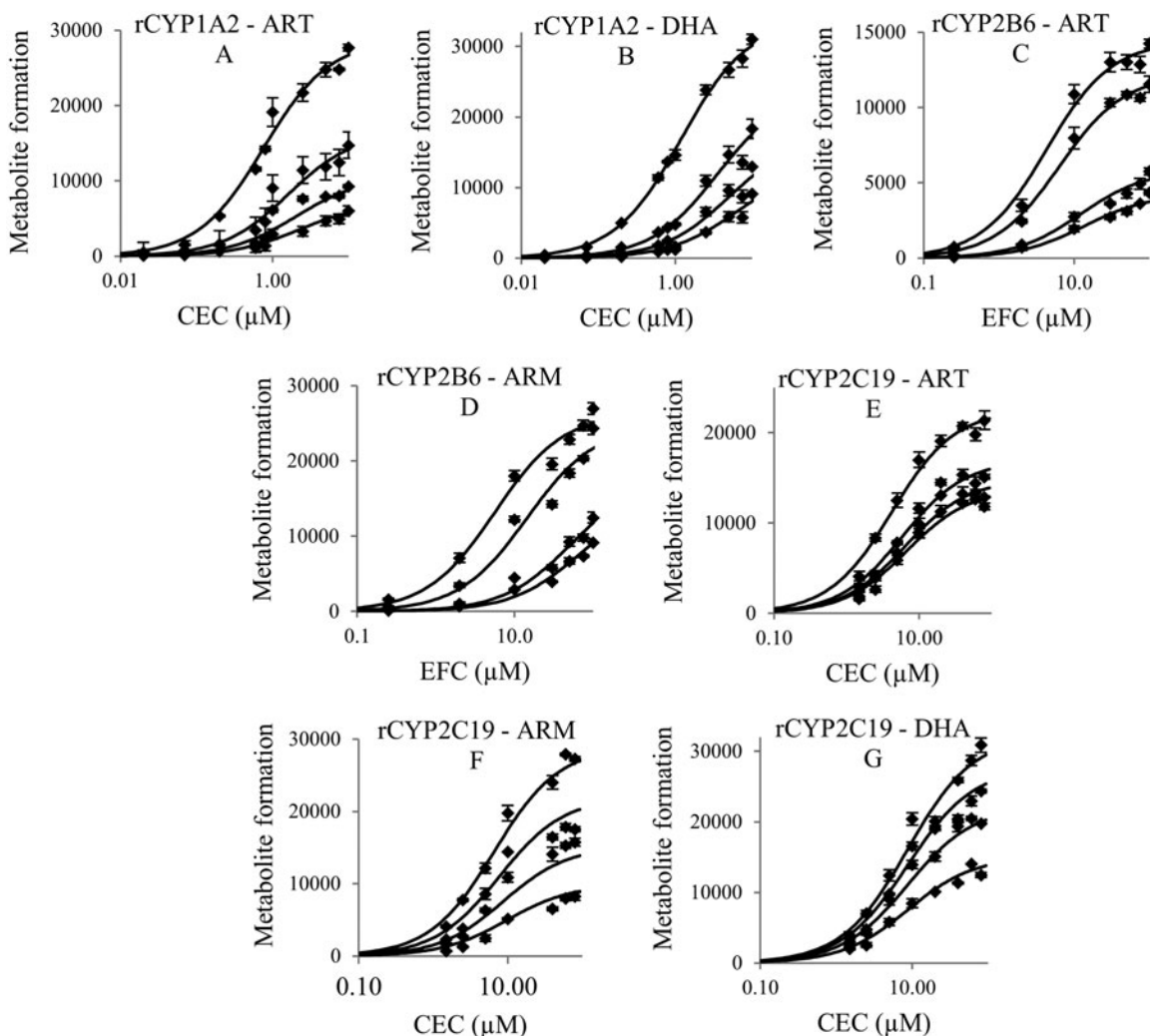


Figure 3. Observed (diamonds) and predicted (lines) formation of fluorescent metabolites (see ‘‘Materials and methods’’), represented by the fluorescence intensity, in recombinant enzymes in the absence and presence of increasing concentrations of artemisinin (ART), artemether (ARM) and dihydroartemisinin (DHA). The predicted inhibition of rCYP1A2 by artemisinin (A) and dihydroartemisinin (B), of rCYP2B6 by artemisinin (C) and artemether (D), and of rCYP2C19 by artemisinin (E) and artemether (F), respectively, are all based on a partial mixed inhibition model (Equation (3)) fitted to the pooled data. The predicted inhibition of rCYP2C19 by dihydroartemisinin (G) is based on a partial noncompetitive inhibition model (Equation (4)). Observed data in the graphs are presented as mean \pm SE ($n = 4$).

Table 6. Enzyme kinetic parameters (K_m , V_{max} and K_i) for artemisinin, artemether and dihydroartemisinin incubated with rCYP1A2, 2B6 and 2C19, respectively, estimated by nonlinear regression analysis. For partial mixed inhibition, the decrease in binding affinity (increased apparent K_m) is described by the term α (>1). The decrease in apparent V_{max} for both partial mixed inhibition and partial noncompetitive inhibition is defined by the term β . Data presented as parameter estimate \pm SE ($n = 4$).

CYP isoform – inhibitor	V_{max}^a	K_m (μM)	K_i (μM)	α	β
CYP1A2 – ART ^b	28.7 ± 0.5	0.8 ± 0.05	1.0 ± 0.1	3.2 ± 0.6	0.17 ± 0.02
CYP1A2 – DHA ^b	33.7 ± 0.6	1.2 ± 0.07	3.4 ± 0.4	5.8 ± 1.2	0.29 ± 0.03
CYP2B6 – ART ^b	14.4 ± 0.3	4.3 ± 0.5	6.2 ± 1.5	3.7 ± 1.1	0.13 ± 0.04
CYP2B6 – ARM ^b	26.4 ± 0.5	5.6 ± 0.6	2.7 ± 0.5	17 ± 7.0	0.38 ± 0.08
CYP2C19 – ART ^b	22.5 ± 0.4	4.2 ± 0.4	1.4 ± 0.3	1.6 ± 0.2	0.58 ± 0.03
CYP2C19 – ARM ^b	28.9 ± 0.7	6.6 ± 0.7	9.1 ± 2.1	1.6 ± 0.4	0.18 ± 0.04
CYP2C19 – DHA ^c	32.3 ± 0.6	8.7 ± 0.5	48.9 ± 9.3	–	0.18 ± 0.06

^aMaximal fluorescence intensity ($\times 10^{-3}$).

^bParameter estimates based on a partial mixed inhibition model (Equation (3)).

^cParameter estimates based on a partial noncompetitive inhibition model (Equation (4)).

on CYP3A4 by artemisinin have been reported by Xing et al. (2012).

It is well accepted that *in vitro* data are essential for understanding a potential enzyme inhibition and DDI *in vivo*,

and potent *in vitro* inhibitors have been demonstrated to cause adverse DDIs in humans (quinidine and CYP2D6, ketoconazole and CYP3A4, etc.; Pelkonen et al., 2008). However, an observed *in vitro* inhibition of a CYP enzyme does not

Table 7. Predicted change in drug exposure and risk for DDI *in vivo* based on own estimated K_i values and the maximum unbound systemic concentrations of inhibitor ($[I]_{\max,u}$) or the maximum unbound concentrations of inhibitors at the inlet to the liver ($[I]_{\max,inlet,u}$) for artemisinin, artemether and dihydroartemisinin on rCYP1A2, 2B6 and 2C19, respectively.

CYP isoform – inhibitor	K_i (μM)	$[I]_{\max,u}$ (μM) ^a	$[I]_{\max,inlet,u}$ (μM) ^a	AUC ratio ^b		Risk for DDI	
				$[I]_{\max,u}$	$[I]_{\max,inlet,u}$		
CYP1A2 – ART	1.0	0.32	5.3	1.3	6.3	High	High
CYP1A2 – DHA	3.4	0.091	0.72	1.0	1.2	Low	Medium
CYP2B6 – ART	6.2	0.32	5.3	1.1	1.9	Medium	Medium
CYP2B6 – ARM	2.7	0.016	0.056	1.0	1.0	Low	Low
CYP2C19 – ART	1.4	0.32	5.3	1.2	4.8	High	High
CYP2C19 – ARM	9.1	0.016	0.056	1.0	1.0	Low	Low
CYP2C19 – DHA	48.9	0.091	0.72	1.0	1.0	Low	Low

^aCalculated based on literature.

^bCalculated based on Equation (2).

necessarily mean that the compound will cause clinically relevant interactions. Many factors influence drug interactions mediated by CYP inhibition, including the contribution of the hepatic clearance to the total clearance of the affected drug, the fraction of the hepatic clearance which is subject to metabolic inhibition, and the ratio of the inhibition constant (K_i) over the *in vivo* concentration of the inhibitor (Ito et al., 1998). The *in vivo* concentration of the inhibitor needs to be high enough for the inhibition to occur, and depending on the therapeutic index of the affected drug, the change in plasma drug concentration caused by the inhibition might be manifested in adverse effects (Pelkonen et al., 2008). The fact that the artemisinin class of endoperoxides has been shown to exert inductive effects on CYP enzymes (Asimus et al., 2007; Elsherbiny et al., 2008; Mihara et al., 1999; Svensson et al., 1998; Xing et al., 2012), makes it hard to predict the clinical relevance of potential inhibitory effects of these drugs on the CYP system. CYP inhibition is considered to be an almost immediate response, and an enzyme inhibition caused by an artemisinin compound would perhaps have an initial effect on the pharmacokinetics of a coadministered drug that is highly metabolized by the affected enzyme. However, if the same enzyme is target for a simultaneous induction, which is a slow process that might affect the plasma concentrations and the efficacy of the coadministered drug in a time-dependent manner, the net inhibition of the enzyme might have little impact on the overall exposure of the coadministered drug. The artemisinin compounds have also been shown to autoinduce their own metabolism, resulting in decreased concentrations and exposure over time (Ashton et al., 1998a; Gordi et al., 2002; Simonsson et al., 2003; van Agtmael et al., 1999a). These factors need to be considered, and therefore the calculated risks of DDIs reported in this study may in some cases be overpredicted. Further support for this statement lies in the fact that the $[I]/K_i$ approach has been reported to overpredict the interaction risk, especially when using $[I]_{\max,inlet,u}$, which has been shown to overestimate the unbound concentration in the liver which actually participated in the inhibition of metabolism (Kanamitsu et al., 2000; Perdaems et al., 2010).

CYP3A4 is the most abundant isoform in the adult human liver and responsible for the oxidative metabolism of the greatest number of drugs that are cleared from the body through hepatic elimination (Pelkonen et al., 2008). CYP3A4 catalyzed reactions are complex and atypical kinetic profiles

have been reported, including substrate-dependent inhibition of the enzyme (Stresser et al., 2000; Turpeinen et al., 2006). The lack of CYP3A4 inhibition with a single probe substrate may be applicable to other probe substrates, but not necessarily. Therefore, it has been suggested that the inhibition of CYP3A4 activity *in vitro* should be identified using multiple substrates (Stresser et al., 2000; Turpeinen et al., 2006). In the current study, the effect of four artemisinin compounds on recombinant CYP3A4 activity were evaluated using the preferred fluorometric substrates BFC and DBF, respectively (Stresser et al., 2000). For the rCYP3A4 catalyzed dealkylation of DBF no effect could be observed for any of the artemisinin compounds tested, while all of them showed a slight activation coupled to an inhibitory response of the dealkylation of BFC as seen in graph H in Figure 1. These opposing results are other important aspects of atypical kinetics and heterotropic effects, namely the occurrence of an effector molecule acting as an enzyme activator at low concentrations while changing to an inhibitor at higher concentrations. Therefore, the behavior of any effector compound (inhibitor, activator, etc.) does not only depend on the substrate that is being metabolized by the affected enzyme, but also on the concentrations of both effector and substrate (Atkins, 2005). In the current study microsomal CYP3A4 activity and the hydroxylation of midazolam, another well-known 3A4 substrate (Pelkonen et al., 2008), were inhibited by artemisinin and artemether, while artesunate and dihydroartemisinin did not affect the enzymatic activity. These findings demonstrate the complexity and the atypical kinetic characteristics of CYP3A4, and the challenge in interpreting how such *in vitro* observations predict the effect *in vivo*.

Most of the identified inhibitory effects exerted by the artemisinin test compounds on the CYP enzymes were best described by the partial mixed inhibition model (Equation (3); $\alpha \neq 1$ and $0 < \beta < 1$). Only the inhibition of CYP1A2 by dihydroartemisinin was described by a partial noncompetitive inhibition model (Equation (4); $\alpha = 1$ and $0 < \beta < 1$). In the present study, inhibition of CYP-mediated reactions is commonly observed to be partial at saturating levels of inhibitor ($0 < \beta < 1$). Partial inhibition has been suggested to be a consequence of the formation of a substrate–inhibitor–enzyme complex that is still active, resulting in an incomplete inhibition of the metabolism of the substrate, even at saturating concentrations of the inhibitor (Atkins, 2005;

Shou et al., 2001). These kinetics can be explained by either the one-site or the two-site model; the former suggesting the inhibitor to bind to the enzyme, thereby preventing the binding of the substrate, and the latter proposing simultaneous binding of both substrate and inhibitor to the enzyme, resulting in partial inhibition due to interactions in the catalytic pocket of the enzyme (Shou et al., 2001).

Conclusions

The data presented in this study show that the artemisinin class of endoperoxides are inhibitors of CYP enzymes *in vitro*, with the most prominent effects on CYP1A2, 2B6, 2C19 and 3A4. Together, these four enzymes are responsible for the clearance mechanisms for 60% of the drugs currently marketed (Zanger et al., 2008). Some of the predicted risks of DDIs *in vivo* reported in the present study are supported by previously published data with respect to CYP1A2. However, the risk of interactions caused by a net inhibition may be overpredicted in some cases due to the ability of artemisinin drugs to induce several CYP isoforms (Asimus et al., 2007; Elsherbiny et al., 2008; Mihara et al., 1999; Svensson et al., 1998; Xing et al., 2012). Furthermore, their ability of artemether and artemisinin to autoinduce their own metabolism, resulting in decreasing exposure over time could have an impact on the inhibitory outcome (Ashton et al., 1998a; Gordi et al., 2002; Simonsson et al., 2003; van Agtmael et al., 1999a).

Declaration of interest

The authors report no declarations of interest.

References

Alin MH, Ashton M, Kihamia CM, et al. (1996). Clinical efficacy and pharmacokinetics of artemisinin monotherapy and in combination with mefloquine in patients with falciparum malaria. *Br J Clin Pharmacol* 41:587–92.

Ashton M, Hai TN, Sy ND, et al. (1998a). Artemisinin pharmacokinetics is time-dependent during repeated oral administration in healthy male adults. *Drug Metab Dispos Biol Fate Chem* 26:25–7.

Ashton M, Nguyen DS, Nguyen VH, et al. (1998b). Artemisinin kinetics and dynamics during oral and rectal treatment of uncomplicated malaria. *Clin Pharmacol Ther* 63:482–93.

Asimus S, Elsherbiny D, Hai TN, et al. (2007). Artemisinin antimalarials moderately affect cytochrome P450 enzyme activity in healthy subjects. *Fundam Clin Pharmacol* 21:307–16.

Atkins WM. (2005). Non-Michaelis–Menten kinetics in cytochrome P450-catalyzed reactions. *Annu Rev Pharmacol Toxicol* 45:291–310.

Augustijns P, D'Hulst A, Van Daele J, Kinget R. (1996). Transport of artemisinin and sodium artesunate in Caco-2 intestinal epithelial cells. *J Pharm Sci* 85:577–9.

Backonja MM, Irving G, Argoff C. (2006). Rational multidrug therapy in the treatment of neuropathic pain. *Curr Pain Headache Rep* 10:34–8.

Bapiro TE, Egnell AC, Hasler JA, Masimirembwa CM. (2001). Application of higher throughput screening (HTS) inhibition assays to evaluate the interaction of antiparasitic drugs with cytochrome P450s. *Drug Metab Dispos Biol Fate Chem* 29:30–5.

Bapiro TE, Sayi J, Hasler JA, et al. (2005). Artemisinin and thiabendazole are potent inhibitors of cytochrome P450 1A2 (CYP1A2) activity in humans. *Eur J Clin Pharmacol* 61:755–61.

Batty KT, Ilett KF, Davis TM. (2004). Protein binding and alpha: beta anomer ratio of dihydroartemisinin *in vivo*. *Br J Clin Pharmacol* 57: 529–33.

Chauret N, Gauthier A, Nicoll-Griffith DA. (1998). Effect of common organic solvents on *in vitro* cytochrome P450-mediated metabolic

activities in human liver microsomes. *Drug Metab Dispos Biol Fate Chem* 26:1–4.

Colussi D, Parisot C, Legay F, Lefevre G. (1999). Binding of artemether and lumefantrine to plasma proteins and erythrocytes. *Eur J Pharm Sci Official J Eur Federation Pharm Sci* 9:9–16.

Elsherbiny DA, Asimus SA, Karlsson MO, et al. (2008). A model based assessment of the CYP2B6 and CYP2C19 inductive properties by artemisinin antimalarials: implications for combination regimens. *J Pharm Pharmacodyn* 35:203–17.

Ericsson T, Masimirembwa C, Abelo A, Ashton M. (2012). The evaluation of CYP2B6 inhibition by artemisinin antimalarials in recombinant enzymes and human liver microsomes. *Drug Metab Lett* 6:247–57.

Ezzet F, Mull R, Karbwang J. (1998). Population pharmacokinetics and therapeutic response of CGP 56697 (artemether + benflumetol) in malaria patients. *Br J Clin Pharmacol* 46:553–61.

FDA (US Food and Drug Administration). (2012). Guidance for industry: drug interaction studies – study design, data analysis, implications for dosing, and labeling recommendations. Silver Spring (MD): US Food and Drug Administration, Center for Drug Evaluation and Research (CDER).

Gordi T, Huong DX, Hai TN, et al. (2002). Artemisinin pharmacokinetics and efficacy in uncomplicated-malaria patients treated with two different dosage regimens. *Antimicrob Agents Chemother* 46: 1026–31.

He F, Bi HC, Xie ZY, et al. (2007). Rapid determination of six metabolites from multiple cytochrome P450 probe substrates in human liver microsome by liquid chromatography/mass spectrometry: application to high-throughput inhibition screening of terpenoids. *Rapid Commun Mass Spectrom* 21:635–43.

Ito K, Brown HS, Houston JB. (2004). Database analyses for the prediction of *in vivo* drug–drug interactions from *in vitro* data. *Br J Clin Pharmacol* 57:473–86.

Ito K, Iwatsubo T, Kanamitsu S, et al. (1998). Quantitative prediction of *in vivo* drug clearance and drug interactions from *in vitro* data on metabolism, together with binding and transport. *Annu Rev Pharmacol Toxicol* 38:461–99.

Kanamitsu S, Ito K, Sugiyama Y. (2000). Quantitative prediction of *in vivo* drug–drug interactions from *in vitro* data based on physiological pharmacokinetics: use of maximum unbound concentration of inhibitor at the inlet to the liver. *Pharm Res* 17:336–43.

Kim MJ, Kim H, Cha JJ, et al. (2005). High-throughput screening of inhibitory potential of nine cytochrome P450 enzymes *in vitro* using liquid chromatography/tandem mass spectrometry. *Rapid Commun Mass Spectrom* 19:2651–8.

Mihara K, Svensson US, Tybring G, et al. (1999). Stereospecific analysis of omeprazole supports artemisinin as a potent inducer of CYP2C19. *Fundam Clin Pharmacol* 13:671–5.

Na-Bangchang K, Krudsood S, Silachamroon U, et al. (2004). The pharmacokinetics of oral dihydroartemisinin and artesunate in healthy Thai volunteers. *Southeast Asian J Trop Med Public Health* 35:575–82.

Pelkonen O, Turpeinen M, Hakkola J, et al. (2008). Inhibition and induction of human cytochrome P450 enzymes: current status. *Arch Toxicol* 82:667–715.

Perdaems N, Blasco H, Vinson C, et al. (2010). Predictions of metabolic drug–drug interactions using physiologically based modelling: two cytochrome P450 3A4 substrates coadministered with ketoconazole or verapamil. *Clin Pharmacokinet* 49:239–58.

Shou M, Lin Y, Lu P, et al. (2001). Enzyme kinetics of cytochrome P450-mediated reactions. *Curr Drug Metab* 2:17–36.

Sidhu JS, Ashton M, Huong NV, et al. (1998). Artemisinin population pharmacokinetics in children and adults with uncomplicated falciparum malaria. *Br J Clin Pharmacol* 45:347–54.

Simonsson US, Jansson B, Hai TN, et al. (2003). Artemisinin autoinduction is caused by involvement of cytochrome P450 2B6 but not 2C9. *Clin Pharmacol Ther* 74:32–43.

Stresser DM. (2004). High-throughput screening of human cytochrome P450 inhibitors using fluorometric substrates. In: Yan Z, Caldwell GW, eds. Optimization in drug-discovery – *in vitro* methods. Spring House (PA): Johnson & Johnson Pharmaceutical Research & Development, 215–30.

Stresser DM, Blanchard AP, Turner SD, et al. (2000). Substrate-dependent modulation of CYP3A4 catalytic activity: analysis of 27 test compounds with four fluorometric substrates. *Drug Metab Dispos Biol Fate Chem* 28:1440–8.

- Svensson US, Ashton M, Trinh NH, et al. (1998). Artemisinin induces omeprazole metabolism in human beings. *Clin Pharmacol Ther* 64: 160–7.
- Turpeinen M, Korhonen LE, Tolonen A, et al. (2006). Cytochrome P450 (CYP) inhibition screening: comparison of three tests. *Eur J Pharm Sci Official J Eur Federation Pharm Sci* 29:130–8.
- van Agtmael MA, Cheng-Qi S, Qing JX, et al. (1999a). Multiple dose pharmacokinetics of artemether in Chinese patients with uncomplicated falciparum malaria. *Int J Antimicrob Agents* 12:151–8.
- van Agtmael MA, Eggelte TA, van Boxtel CJ. (1999b). Artemisinin drugs in the treatment of malaria: from medicinal herb to registered medication. *Trends Pharmacol Sci* 20:199–205.
- White NJ, van Vugt M, Ezzet F. (1999). Clinical pharmacokinetics and pharmacodynamics and pharmacodynamics of artemether-lumefantrine. *Clin Pharmacokinet* 37:105–25.
- WHO (World Health Organization). (2010). Guidelines for the treatment of malaria, 2nd ed. Geneva, Switzerland: World Health Organization.
- Xing J, Kirby BJ, Whittington D, et al. (2012). Evaluation of P450 inhibition and induction by artemisinin antimalarials in human liver microsomes and primary human hepatocytes. *Drug Metab Dispos Biol Fate Chem* 40:1757–64.
- Zanger UM, Turpeinen M, Klein K, Schwab M. (2008). Functional pharmacogenetics/genomics of human cytochromes P450 involved in drug biotransformation. *Anal Bioanal Chem* 392:1093–108.

Supplementary material available online
Supplemental information Figures